Hindawi Publishing Corporation
International Journal of Electrochemistry
Volume 2014, Article ID 304296, 12 pages
http://dx.doi.org/10.1155/2014/304296

Research Article

Selection of the Best Process Stream to Remove Ca^{2+} Ion Using Electrodialysis from Sugar Solution

Jogi Ganesh Dattatreya Tadimeti,[1] Shilpi Jain,[1] Sujay Chattopadhyay,[1] and Prashant Kumar Bhattacharya[2]

[1]*Polymer and Process Engineering Department, IIT Roorkee, Saharanpur Campus, Saharanpur 247 001, India*
[2]*Chemical Engineering Department, Indian Institute of Technology, Kanpur 208 016, India*

Correspondence should be addressed to Sujay Chattopadhyay; sujay1999@gmail.com

Received 30 July 2014; Revised 3 November 2014; Accepted 14 November 2014; Published 14 December 2014

Academic Editor: Sergio Ferro

Electrodialytic removal of calcium chloride ($CaCl_2$, 25–50 mol·m^{-3}) from 5% sugar solution was executed in batch recirculation mode. Calcium ion removal rate was monitored with (i) applied potential, (ii) feed flow rate, (iii) solution viscosity and conductivity, and (iv) catholyte streams (NaOH or sodium salt of ethylene diamine tetraacetic acid-acetic acid, Na_2EDTA-AA). Unsteady state model for ion concentration change was written for the ED cell used. Linearized Nernst-Planck equation instead of Ohm's law was applied to closely obtain the current density and concentration change theoretically. The model developed could closely predict the experimental observation. Mass transfer coefficients and specific energy densities were estimated for each combination of catholyte stream used. NaOH showed better performance for a short duration over Na_2EDTA-acetic acid combination.

1. Introduction

In cane based sugar industry the sugar concentration in the extracted juice after lime ($CaO + H_2O$) treatment and color removal (clarification step) usually reaches around 5% (mass basis). This stream subsequently enters into series of evaporators to get concentrated. Presence of excess calcium in the postfloculation and precipitation stage of clarified sugar juice creates series of nuisance [1] to the subsequent stages (evaporators, etc.) in sugar industries affecting product quality as follows.

(1) Scale formation in the evaporators.
(2) Improper crystallization.
(3) Molasses percentage may increase due to inversion of sugar in alkaline medium.
(4) Storage is hampered because of hygroscopic nature of these metals ions.
(5) Excess calcium is not hygienic as well.

Therefore, removal of it at appropriate stage would drastically reduce operation and maintenance (evaporator scaling) cost and improve product quality. Electrodialysis (ED) was chosen to remove $CaCl_2$ from its sugar solution. ED was applied earlier in sugar industry to recover tartrate and malate from grape sugar [2] and in demineralisation of beet sugar syrup, juice, and molasses [3, 4]. The technological difficulties arise due to fouling of ion exchange membranes mainly due to deposition of organic/inorganic molecules (sugars, proteins, Ca^{2+}, Mg^{2+}, etc.). With increase in solution viscosity fouling becomes even severe and affects the current efficiency and ion removal rate. The concentration polarization occurs around membrane surface leading to increase in ion resistance, and this is minimized with the help of suitable spacer design, temperature, pH, and flow rates applied [5–11].

A batch recirculation ED process having a single diluate channel was performed to remove the $CaCl_2$ from sugar solution. As reported elsewhere [5] during ED process concentration polarization arises around the membrane which limits

the net salt transport. This issue was taken up and sorted out using different combination of anolyte and catholyte streams. Different electrolyte streams (NaOH, acetic acid-Na_2EDTA mixture) were selected as catholyte keeping anolyte as HCl solution.

In a batch mode electrodialysis with continuous recirculation of feed stream, properties like electrolyte concentration of diluate (feed tank), concentration profiles around that membrane, and all physical properties of the solution change with time. The effect of all these parameters is reflected in ion removal rate and current density of the ED cell. Therefore, an unsteady state model that can closely predict the ion removal rate and overall current density will be quite relevant in application point of view. Nernst-Planck equation (purely based on first principles) and irreversible thermodynamics were used to estimate current density and ion concentration [12].

2. Materials and Methods

2.1. Equipment

2.1.1. Electrodialysis Setup. The experimental setup used for ED application is shown in the Figure 1 [13]. The ED cell and setup were from Berghof, Germany. The electric field was applied across the cell stack by a built-in D.C. source. Voltage and current between the two electrodes were measured by a built-in digital voltmeter and ammeter, respectively. The ED cell consisted of three compartments as shown in the figure. Membranes used were obtained from Permionics, Gujarat, and cross-linked styrene and di-vinyl benzene gel was used as base material. Cation exchange membrane (CEM) separates the cathode compartment and anion exchange membrane (AEM) separates the anode compartment from the feed chamber. The effective membrane area for the cell, A_m, was 0.0037 m^2 and the feed compartment thickness, h, was 0.002 m.

2.1.2. Power Supply. The power supply was provided through a voltage stabilizer of 110/220 V A.C. with 50–80 Hz frequency. The same gave an output voltage 0–49.9 V DC and current 0–3.99 A. Four centrifugal pumps were inbuilt with the system for pumping the solution.

2.1.3. Conductivity Meter. Solution conductivity was noted at regular interval through an offline conductivity meter (Systronics India) of 200 mMho with 5 ranges (accuracy ±1%).

2.1.4. ED Cell Compartments and Solutions Used. 1000 mL solutions of each stream (feed, catholyte, and anolyte) were taken in three chambers (Figure 1), respectively. Each chamber was connected with the respective three compartments of the ED cell through flexi tubing. Solutions were circulated at a constant rate by three centrifugal pumps and the solution flow rates were measured using rotameters connected to each stream. Table 1 indicates membrane parameters obtained from Permionics India Ltd. The composition and flow rates of three streams used are reported in Table 2.

Synthetic solution of 5% sugar and calcium chloride ($CaCl_2$) was prepared in distilled water. The concentration of sugar was kept unchanged but that of $CaCl_2$ was varied. The synthetic solution having $CaCl_2$ with initial concentrations of 25 mol·m^{-3} and 50 mol·m^{-3} were used in the diluate channel of ED cell. Dilute solution of HCl (100 mol·m^{-3}) was used as anolyte in all experiments while NaOH (100 mol·m^{-3}) was used as catholyte in experiment 1 and equimolar mixtures of acetic acid (AA) and Na_2EDTA (25 mol·m^{-3} and 50 mol·m^{-3}) were, respectively, used as catholyte in experiments 2 and 3 (Table 2).

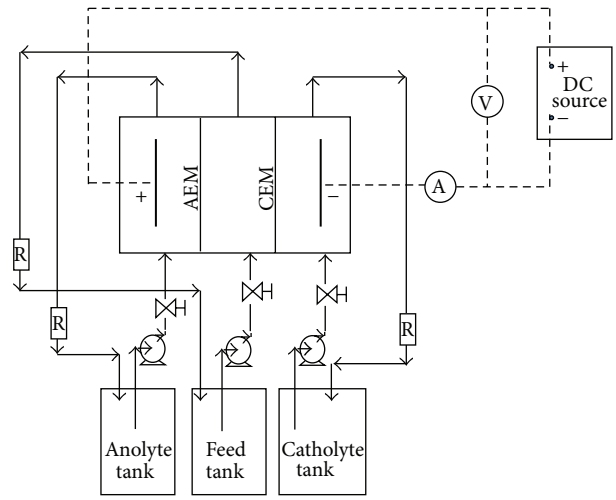

Figure 1: Batch recirculation electrodialysis process showing the storage tanks, pumps, manual control valves, various chambers of the ED cell, electrodes, DC supply source, voltmeter, ammeter, and flow meters used in the experiment [13].

Table 1: Membrane parameters as obtained from Permionics India Ltd.

Physical parameters	Cation exchange membrane	Anion exchange membrane
Transport number	0.91	0.9
Experimental resistance (ohm cm^{-2})	2.0–3.5	—
Max. pressure allowed ($kgcm^{-2}$)	3.0	3.0
Thickness (mm)	0.11 to 0.15	0.09–0.11
Max. temperature (°C)	60	60

2.1.5. Viscosity Measurement. Viscosity measurement was carried out using Ubbelhood viscometer always fitted in a constant temperature bath to nullify any temperature effect on capillary flow.

2.2. Procedure. The chambers of the ED cell and membranes were washed thoroughly before each experiment was carried out. Initially, the feed solution containing 5% sugar and $CaCl_2$

Table 2: Different process variables chosen during ED experimentation [13].

Expt. number	Feed solution	Feed flow rate ($mL \cdot min^{-1}$)	Anolyte solution	Anolyte flow rate ($mL \cdot min^{-1}$)	Catholyte solution	Catholyte flow rate ($mL \cdot min^{-1}$)	Voltage applied (V)	Time (min)
1	25 $mol \cdot m^{-3}$ $CaCl_2$ in 5% sugar solution	130	100 $mol \cdot m^{-3}$ HCl solution	830	100 $mol \cdot m^{-3}$ NaOH solution	830	4	685
2	25 $mol \cdot m^{-3}$ $CaCl_2$ in 5% sugar solution	130	100 $mol \cdot m^{-3}$ HCl solution	830	25 $mol \cdot m^{-3}$ Na_2EDTA + 25 $mol \cdot m^{-3}$ AA solution	830	4	240
3	50 $mol \cdot m^{-3}$ $CaCl_2$ in 5% sugar solution	130	100 $mol \cdot m^{-3}$ HCl solution	830	50 $mol \cdot m^{-3}$ Na_2EDTA + 50 $mol \cdot m^{-3}$ AA solution	830	4	240

was used and was circulated at a constant rate (130 mL/min) through the feed compartment. The feed solution, anolyte, and catholyte were continuously recycled through the ED cell and that caused a continuous change in salt concentration of feed solution. The concentration was measured at regular intervals. For a fixed applied voltage (V), variation of current ("I" through the membrane stack) and concentration of salt (Ca^{2+} ions) was estimated from conductivity measurement and using standard calibration chart (mass concentration versus conductance) and was recorded with time (t).

ED cell was dismantled; membranes were taken out, checked visually to find any deposition over the surfaces after each experiment. Membranes were then washed with distilled water and oven dried at 100°C for 24 hours and weighed to find any gain or loss in mass of membrane.

3. Modeling of Ion Transport

Current density and limiting current density (LCD) of an ED cell is a function of a series of parameters, for example, physical (cell geometry, flow dynamics, spacer spacing, solution density, and viscosity) and chemical (ion concentration, transport number, and diffusivity) for a given set of membrane pairs. Precise estimate of these parameters and application of Nernst-Planck equation (assuming zero ion concentration on the membrane surface) would give a theoretical estimate of LCD which can also be determined experimentally from plot of I versus V characteristics of the electrolyte in the ED cell [7, 9].

3.1. Determination of Bulk Concentration of Diluate Compartment. Concentration of ions was obtained through unsteady mass balance over diluate, catholyte, and anolyte compartments. The following assumptions were made [18].

(i) The ED cell and the feed tank are approximated to be a perfectly mixed flow reactor.

(ii) Back diffusion of ions was ignored.

(iii) Electroneutrality condition is always maintained.

The mass balance equation of diluate compartment in the ED cell can be expressed as

$$V_{\text{dilC}} \frac{dC^{\text{dil}}}{dt} = Q^{\text{dil}} \left(C_T^{\text{dil}} - C^{\text{dil}}\right) - \frac{\eta i A_m}{zF}, \quad (1)$$

where V_{dilC} is the volume of the diluate compartment (m^3) and t is time (s), C_T^{dil} and C^{dil} represent diluate concentrations leaving feed tank and leaving cell compartment ($mol \cdot m^{-3}$), Q^{dil} is the diluate volumetric flow rate (m^3/s), η is the current efficiency, i is the current density ($A \cdot m^{-2}$), and A_m is the effective membrane area (m^2).

η can be obtained from the following equation [18, 19]:

$$\eta = t_{+,\text{CEM}} + t_{-,\text{AEM}} - 1, \quad (2)$$

where $t_{+,\text{CEM}}$ is the transport number of cation in cation exchange membranes and $t_{-,\text{AEM}}$ is the transport number of anion in anion exchange membrane.

Similarly, unsteady state mass balance around feed tank can be written as

$$\frac{d\left(V_T C_T^{\text{dil}}\right)}{dt} = Q^{\text{dil}} \left(C^{\text{dil}} - C_T^{\text{dil}}\right), \quad (3)$$

where V_T is the volume of feed tank (m^3). During electrodialysis water transport occurs across the membranes due to electroosmosis and osmosis [19]. Volume change (due to water transport) was ignored as there was no net volume change noted experimentally.

3.2. Determination of the Current Density

3.2.1. Overall Flux Equation. A pictorial representation of different concentration profiles possibly developed around the membrane is described in Figure 2. The flux of ions passing through the membrane can be expressed by generalized Nernst Planck equation as [7]

$$N_j = -D_j \frac{\partial C_j}{\partial x} - \frac{z_j C_j F D_j}{RT} \frac{\partial \psi}{\partial x}, \quad (4)$$

where x is the distance measured from boundary layer in contact with the bulk solution in diluate channel towards the membrane, D_j is the diffusivity of ion ($m^2 \cdot s^{-1}$), C_j is the concentration of ion j ($mol \cdot m^{-3}$), R is the universal gas constant (8.314 $J \cdot mol^{-1} \cdot k^{-1}$), T is the temperature (K), z_j is the charge of diffusing species j, and $\partial\psi/\partial x$ is the potential gradient ($V \cdot m^{-1}$) and F is the Faraday constant ($C \cdot geqv^{-1}$).

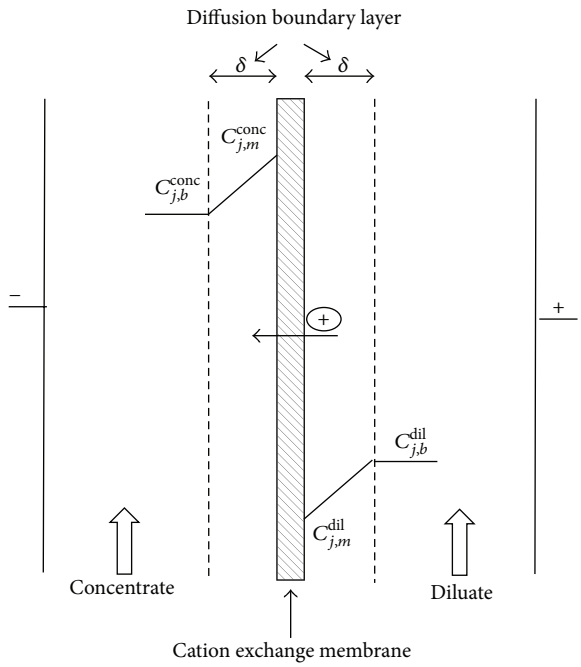

Figure 2: Depiction of ion transport and hypothetical linear concentration boundary layer formed across either side of the membrane in ED cell.

The total molar flux of ion "j" through the ion exchange membrane, $N_{j,m}$, can be related to the current density, i, as [7]

$$N_{j,m} = \frac{t_{j,m} i}{z_j F}, \tag{5}$$

where $t_{j,m}$ is the transport number of ion j in the membrane, i is current per unit area of membrane or current density ($A \cdot m^{-2}$), and z_j is the charge of the ion.

At steady state N_j and $N_{j,m}$ are equal; that is,

$$\frac{t_{j,m} i}{z_j F} = -D_j \frac{\partial C_j}{\partial x} - \frac{z_j C_j F D_j}{RT} \frac{\partial \psi}{\partial x}. \tag{6}$$

Assuming that a linear profile of the concentration distribution exists along the boundary layer, the linearized Nernst-Planck equation could be used instead of (6). Expression for the linearized Nernst-Planck equation when applied in the diluate chamber is [7]

$$\frac{t_{j,m} i}{z_j F} = \frac{D_j \left(C^{dil}_{j,b} - C^{dil}_{j,m}\right)}{\delta} - \frac{z_j D_j F \xi C^{dil}_{j,m}}{RT}, \tag{7}$$

where δ is the boundary layer thickness (m), $C^{dil}_{j,b}$ and $C^{dil}_{j,m}$ are concentrations of ions in bulk and at the membrane surface, respectively, of the diluate compartment, and ξ is the potential gradient ($V \cdot m^{-1}$) and is expressed as

$$\xi = \frac{\psi}{\delta}. \tag{8}$$

In (7) the first part, that is, $D_j(C^{dil}_{j,b} - C^{dil}_{j,m})/\delta$, denotes flux due to molecular diffusion flux of ion arising out of concentration variation between solution bulk and boundary layer over membrane surface. The second part, that is, $z_j D_j F \xi C^{dil}_{j,m}/RT$, shows flux due to externally applied potential over the membrane.

3.2.2. Boundary Layer Thickness, δ Estimation. δ is estimated using film theory (equation (9)) and salt mass-transfer coefficient [7, 20]. Salt mass-transfer coefficient is usually determined based on salt diffusivity and suitable mass-transfer correlation, which in-turn is dependent on flow profile and physical properties of the fluids, cell geometry, and surface morphology of membranes used in ED cell [7, 9, 21, 22]:

$$\delta = \frac{D_j}{k}, \tag{9}$$

where, D_j and k are diffusivity and mass transfer coefficient of diffusing species in solution. Each of these parameters was separately estimated using standard correlations. The mass transfer coefficient was obtained from Sherwood number [7, 20, 21] as:

$$\mathrm{Sh} = \frac{k \cdot l}{D_j}, \tag{10}$$

where l is the characteristic length (m). Sherwood number, Sh, is expressed as a function of Reynolds number, Re, and Schmidt number, Sc [7, 20]. The empirical expression of Sherwood number is based on cell geometry and spacer configuration chosen for the present cell as indicated in the following [17, 20, 23]:

$$\mathrm{Sh} = a \cdot \mathrm{Re}^b \cdot \mathrm{Sc}^c, \tag{11}$$

where Sc (Schmidt number, $\mu/\rho D_j$) is estimated from physical properties (viscosity and density) of the medium while Reynolds number ($\rho v l/\mu$) indicates flow characteristics of the medium and channel spacing as "l" and a, b, c are the empirical constants, which are determined by fitting the data ($\mathrm{Sh}/\mathrm{Sc}^c$ versus Re) for experiments where flow rate is varied. In this work, the values of a, b, and c are taken from literature [17] and are given in Table 3.

Ionic diffusivity is entirely dependent on the size of hydrodynamic diameter of ions. Assuming infinite dilution this ionic diffusivity is estimated using the Nernst-Haskel equation (12) [14] as

$$D^{\circ} = \frac{RT\left[\left(1/z_+\right) + \left(1/z_-\right)\right]}{F^2\left[\left(1/\lambda_+\right) + \left(1/\lambda_-\right)\right]}, \tag{12}$$

where z_+ and z_- denote charges of cation and anion, respectively, while λ_+ and λ_- denote limiting ionic conductance in the solvent. Other parameters bearing meaning and units are as reported in the nomenclature.

Table 3: Values of different physical parameters used in the model.

Parameter	Value	Reference
Temperature, T	298 K	This work
Transport number of the cation in CEM, $t_{+,\mathrm{CEM}}$	0.91	Table 1
Transport number of the anion in AEM, $t_{-,\mathrm{AEM}}$	0.9	Table 1
Transport number of cation in the solution, $t_{\mathrm{Ca}^{2+},s}$	0.4387	This work [7]
Transport number of anion in the solution, $t_{\mathrm{Cl}^{-},s}$	0.5613	This work [7]
Diffusivity of $CaCl_2$ in 5% sugar solution at 25°C, $D_{\mathrm{CaCl_2}}$	1.198×10^{-9} m^2·s^{-1}	This work [14, 15]
Diffusivity of Ca^{2+} ions at infinite dilution and at 25°C, $D^{\circ}_{\mathrm{Ca}^{2+}}$	7.92×10^{-10} m^2·s^{-1}	This work [14]
Diffusivity of Ca^{2+} ions in 5% sugar solutions at 25°C, $D_{\mathrm{Ca}^{2+}}$	7.11×10^{-10} m^2·s^{-1}	This work [14, 15]
Diffusivity of Cl^- ions in 5% sugar solutions at 25°C, D_{Cl^-}	18.2×10^{-10} m^2·s^{-1}	This work [14, 15]
Distance between adjacent membranes, l	2×10^{-3} m	This work
Area of the membrane, A_m	3.7×10^{-3} m^2	This work
Charge on the calcium ion, $z_{\mathrm{Ca}^{2+}}$	+2	This work
Viscosity of 5% sugar solution, μ	9.92×10^{-4} Pa·s	[16]
Velocity of the feed stream, v	3.1×10^{-2} m·s^{-1}	This work
Applied voltage, E_{tot}	4 V	This work
Current density initial value, $i(0)$	122 A·m^{-2}	This work
Current efficiency, η	0.81	This work
Sh number empirical equation constant, a	0.46 for catholyte NaOH	[17]
	0.25 ± 0.03 for catholyte AA-Na_2EDTA	This work
Sh number empirical equation constant, b	0.63 for any anolyte and catholyte	[17]
Sh number empirical equation constant, c	0.33 for any anolyte and catholyte	[17]

Diffusivity is a strong function of viscosity which was corrected using equation proposed by Yuan-Hui and Gregory [15]

$$\frac{D}{D^{\circ}} = \frac{\mu^{\circ}}{\mu}. \tag{13}$$

3.2.3. Estimation of Membrane Surface Concentration. The membrane surface concentration of ions is dependent on current density under an applied voltage. As long as the ED operation is executed below limiting current (surface concentration becomes zero), the surface concentration on either side can be estimated from bulk concentration measurement (diluate/concentrate), current density, and limiting current density using (14) and (15) [19, 24]:

$$C^{\mathrm{conc}}_{j,m} = C^{\mathrm{conc}}_{j,b}\left(1 + \frac{i}{i_{j,\mathrm{lim}}}\right), \tag{14}$$

$$C^{\mathrm{dil}}_{j,m} = C^{\mathrm{dil}}_{j,b}\left(1 - \frac{i}{i_{j,\mathrm{lim}}}\right), \tag{15}$$

where $C^{\mathrm{conc}}_{j,m}$ and $C^{\mathrm{conc}}_{j,b}$ are the concentrations of ion j, on the membrane surface and in bulk of the concentrate compartment, respectively, in the ED cell. $C^{\mathrm{dil}}_{j,m}$ and $C^{\mathrm{dil}}_{j,b}$ are the concentrations of ion j, on the membrane surface and in the bulk of the diluate side, respectively, in the ED cell.

3.2.4. Estimation of Current Density and Limiting Current Density (i and $i_{j,lim}$). LCD (of a single electrolyte) is estimated using the following equation [5, 9]:

$$i_{j,\mathrm{lim}} = \frac{C^{\mathrm{dil}}_{j,b} D_j z_j F}{\delta\left(t_{j,m} - t_{j,b}\right)}, \tag{16}$$

where $t_{j,m}$ and $t_{j,b}$ are transport numbers of ion j in membrane and electrolyte solution, respectively.

Considering ion flux in the diluate side of the IEM, (15) is used to calculate concentration of ion j, at the membrane surface of diluate side $C^{\mathrm{dil}}_{j,m}$.

The current density can be expressed by (17) after substitution of (15) and (16) in (6):

$$i = \left(C^{\mathrm{dil}}_{j,b} D_j z_j \xi \frac{F}{RT}\right) \times \left(\frac{t_{j,m} - t_{j,b}}{z_j F} + \frac{\xi\delta\left(t_{j,m} - t_{j,b}\right)}{RT} - \frac{t_{j,m} z_j}{F}\right)^{-1}, \tag{17}$$

where ξ the potential gradient can be estimated from Nernst equation given as follows [18, 19]:

$$\xi = -\left(2t_{j,m} - 1\right)\frac{RT}{\delta F}\ln\left(\frac{\gamma^{\mathrm{dil}}_b C^{\mathrm{dil}}_{j,b}}{\gamma^{\mathrm{dil}}_m C^{\mathrm{dil}}_{j,m}}\right), \tag{18}$$

where γ^{dil}_m and γ^{dil}_b are the mean ionic activity coefficients corresponding to the ions at the wall of IEM and in the bulk

of solution, respectively, within the diluate channel and they can be estimated using Debye-Huckel limiting law [25].

4. Numerical Estimation of Parameters

The sequence of steps followed to obtain theoretical estimate of concentration variation is described using flow chart (Figure 3). The differential equations (1) and (3) were integrated using Euler method with 1 s time step. Few crucial parameters and their evaluation method are presented below.

4.1. Determination of Transport Number of Ion in Solution. Bulk transport number $t_{j,b}$ is the fraction of total current carried by the ion type which is a function of diffusion coefficient and ionic mobility of hydrated species. Ions in solution get hydrated with solvent molecules and difference in hydration ability causes variation in size, diffusivity, and mobility of such species. Thus, ions do not transport current equally in solution. The transport number was estimated using following equation [7]:

$$t_{j,b} = \frac{|z_j| D_j}{\sum_{j=1}^{n} |z_j| D_j}. \quad (19)$$

For a binary-ion salt solution, $n = 2$, $j = 1$ for cation and $j = 2$ for anion, respectively.

4.2. Determination of Current from Resistance Measurement. Initial current density estimation is essential to obtain salt concentration at membrane surface and start numerical integration which may be evaluated either experimentally or from applied potential and solution resistance using Ohm's law. The potential applied may be expressed as

$$E_{\text{tot}} - E_{\text{el}} = R_{\text{tot}} \cdot J, \quad (20)$$

where E_{el} is the potential drop near the electrodes, R_{tot} is the overall resistance (ohm) of the ED cell, and J is the current (A). The overall resistance is the sum of resistances of individual chambers:

$$R_{\text{tot}} = R_{\text{anolyte}} + R_{\text{diluate}} + R_{\text{catholyte}}, \quad (21)$$

where resistance of anolyte, catholyte, and diluate channel are determined either directly from conductivity measurement or from extended Kohlrausch-equation [19, 25]. The conductivity and the resistance are related as

$$\text{Resistance} = \frac{1}{\Lambda} \frac{L}{A_m}, \quad (22)$$

where Λ is the conductivity of solution (mho·m^{-1}), L is the gap between membranes or the compartment thickness (m), and A_m is the effective membrane area (m^2).

4.3. Determination of Specific Energy Consumption. The specific energy consumption, E_{sp} (kWh·kg^{-1}), was obtained using the following equation:

$$E_{\text{sp}} = \frac{\int_{t_1}^{t_2} \varepsilon A_m i(t)\, dt}{M_{\text{CaCl}_2} \Delta n_{\text{CaCl}_2}(t)}, \quad (23)$$

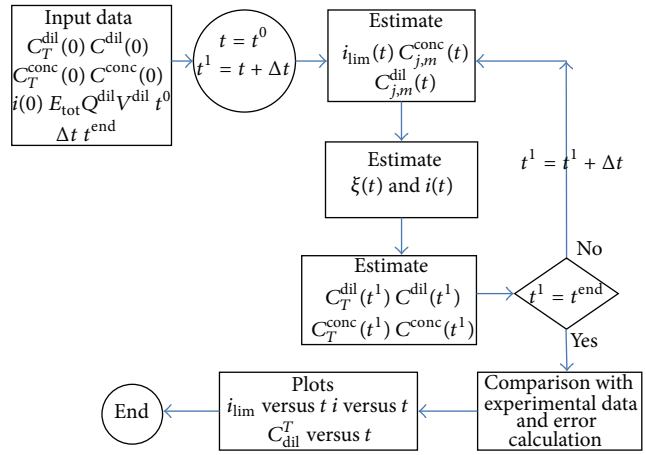

Figure 3: MATLAB program algorithm showing calculation steps followed to estimate process parameters.

where ε is the applied potential in V, A_m is the area of the membrane in m^2, $i(t)$ is the current density as a function of time in A·m^{-2}, M_{CaCl_2} is the molecular mass of $CaCl_2$ (=111.02 g/mol), and $\Delta n_{\text{CaCl}_2}(t)$ is the number of moles of $CaCl_2$ removed from the feed solution at various time intervals.

5. Results and Discussions

5.1. Role of Sugar and $CaCl_2$ Concentration on Solution Viscosity and Influence of Temperature. Sugar solution viscosity increases nonlinearly (Figure 4) with increase in sugar concentration (5 to 20 wt%). Viscosity values range between 0.72 and 1.5 mPa·s with increase in sugar concentration. These values were very much comparable with the literature reported data [16]. Solution viscosity does not show any appreciable change with $CaCl_2$ concentration (0–50 mol/m^3) (Figure 5). Influence of temperature on $CaCl_2$ solution viscosity was recorded at 20, 25, 32, 37, and 42°C and viscosity decreases between 1.22 and 0.7 mPa·s. Nearly ~43% lowering in solution viscosity with temperature rise between 20 and 42°C is noted in Figure 5.

5.2. Role of Sugar and $CaCl_2$ Concentration on Electrical Conductivity of Electrolyte. Figure 6 shows plot of $CaCl_2$ concentration on the electrical conductivity, which was estimated in presence and absence of sugar. Electrical conductivity increases almost linearly with rise in $CaCl_2$ concentration (5 to 50 mol·m^{-3}). The $CaCl_2$, being a strong electrolyte, dissociates completely in solution, thus increasing number of ions per unit volume available for ionic conductance. On the contrary, sugar addition dampens the conductivity value. This is possibly because sugar is a water soluble nonelectrolyte which does not change the number of ionic species responsible for current carriage; thus, presence of inert sugar molecules basically increases crowding in solution.

5.3. Effect of Applied Potential on Ion-Removal Rate. The applied potential is a crucial parameter to define removal

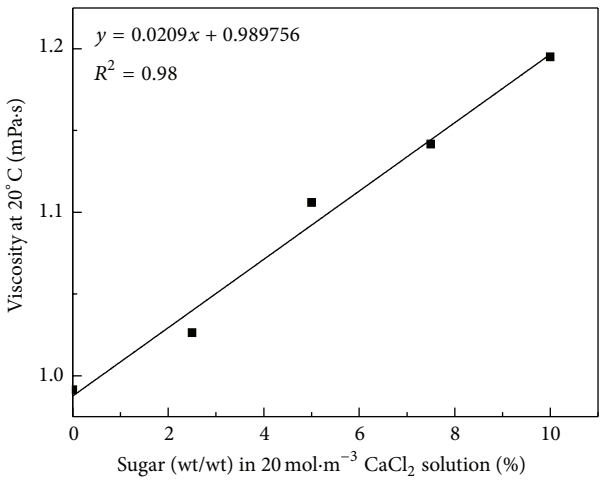

Figure 4: Effect of wt% of sugar on solution viscosity at 20°C.

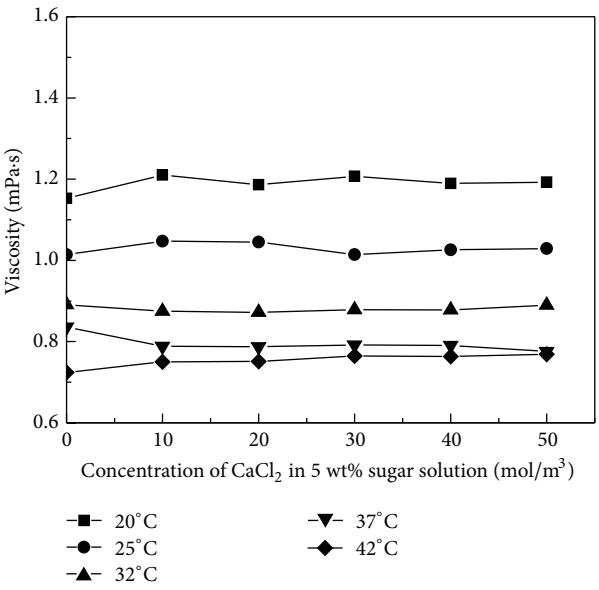

Figure 5: Effect of concentration of $CaCl_2$ in 5 wt% sugar solution on solution viscosity at different temperatures.

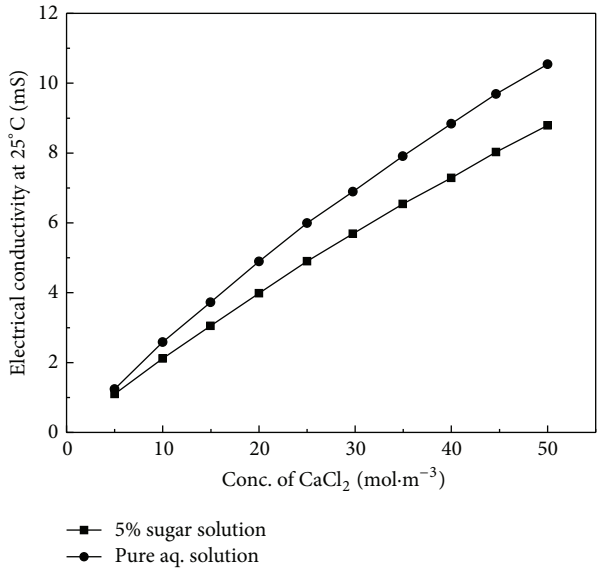

Figure 6: Effect of molar concentration of $CaCl_2$ in water with and without sugar on electrical conductivity of solution.

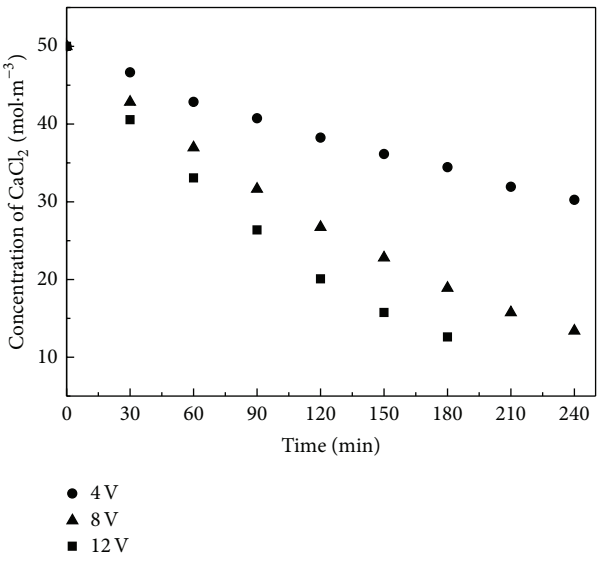

Figure 7: Effect of applied potential on the feed concentration. Process conditions are feed: 130 mL/min with $CaCl_2$ (50 mol·m^{-3}) in 5 wt% sugar solution; anolyte: 830 mL/min with HCl (100 mol·m^{-3}); catholyte: 830 mL/min with Na_2EDTA (50 mol·m^{-3}) + AA (50 mol·m^{-3}); applied voltage: 4 V, 8 V and 12 V.

rate and efficiency. With increased potential, ion removal rate increases causing rapid lowering of batch time [26]. In a batch operation, with gradual lowering of ion concentration the current density keeps dropping. Once, the concentration reaches below limiting value the solution resistance becomes very high and heating starts. At this increased temperature electrolysis of water starts and a major portion of applied potential gets consumed without much gain in ion removal. Thus, overall energy consumption increases affecting process efficiency [5, 22].

Three different voltages (4 V, 8 V, and 12 V) were applied keeping other process parameters unchanged. Figure 7 shows effect of applied potential on Ca^{2+} ion removal rate. With higher potential, the ion removal rate increases. This is quite obvious because with increased electrical driving force (potential), more current passes through the solution as long as resistance remains unchanged. It is interesting to note that at lower potential, the ion removal rate remains linear for a long duration (>240 min) indicating Ohm's law might be applicable. This is not observed with higher potentials. With −8 V, the nonlinearity appears at time ~180 min while the same happens at time ~120 min for −12 V. Possibly unwanted electrode reactions (water splitting) initiate at early stages with increased potential. This certainly influences the ion removal rate showing variation in slope of the concentration

drop curve. This indicates that at higher voltage rapid depletion of ions and a nonlinear rise in resistance occurs. Rapid nonlinear rise in solution resistance was also observed earlier by different scientists [8, 9].

5.4. Effect of Flow Rate on Ion Removal Rate. Change in ion removal rate with variation in feed flow rate, without disturbing catholyte and anolyte streams conditions (flow rate, components, concentration, etc.), was analyzed and reported in Figure 8. Feed flow rates were varied as 80, 130, and 180 mL/min and change in ion removal rate was noted after nearly 60 min of ED operation. A slow rise in removal rate with increased flow rate was observed. Increased flow rate possibly increased turbulence which reduced thickness of stationary boundary film over membrane surface. This lowered the overall ion transfer resistance and increased ion removal rate.

5.5. Model Prediction of Experimental "i" and Ca^{2+} Ion Concentration. The batch mode of electrodialysis with continuous recirculation under an applied potential becomes an unsteady state process. The electrolyte concentrations of diluate (feed tank) and concentrate streams, solution resistance (conductivity), concentration profile around membrane, and bulk physical properties of the solution become time dependent. The cumulative effects of all these parameters are reflected in diluate (feed tank) concentration and overall current density of the ED cell. Therefore, the mathematical model emphasizes two crucial parameters: (i) electrolyte ($CaCl_2$) concentration of the diluate stream (feed tank) and (ii) overall current density of the cell. Unsteady state mass balance around the diluate channel/tank is written in terms of important process variables, for example, vessel volume, flow rate, concentration, current density, current efficiency, and membrane area. Nernst Planck equation and irreversible thermodynamics are used to estimate the ionic flux through the boundary layer over the membrane. The model proposed closely predicts experimental data between the chosen range of process condition of Ca^{2+} ion (Figures 9 and 10) and current density with time (Figure 9) in the ED cell.

Molar concentration of the recirculating feed solution was obtained by solving coupled differential equations. Equations (1) and (3) and physical process parameters values are listed in Table 3. Solution steps (using MATLAB code) are discussed in Figure 3. The concentration estimates so obtained were used to estimate current density, i (17). The theoretical model could closely predict the experimental data (Experiments 1, 2, and 3) of concentration variation (Figures 9 and 10). Experiments 2 and 3, performed with two different concentrations of $CaCl_2$ (25 and 50 mol·m^{-3}) in feed solution, behaved in the same manner (Figure 10). This supports the fact that the method adopted in concentration estimation was correct and reproducible.

Initially solute concentration (25 mol·m^{-3}) of the feed solution drops steadily in experiment 1, the rate of which slows down after nearly 200 min (Figure 9). The experimental current density also follows same trend (Figure 9). A steady drop in current density from 120 A·m^{-2} to 40 A·m^{-2} during first 200 min was recorded possibly due to rapid lowering in ionic concentration in the diluate under applied potential of 4 V.

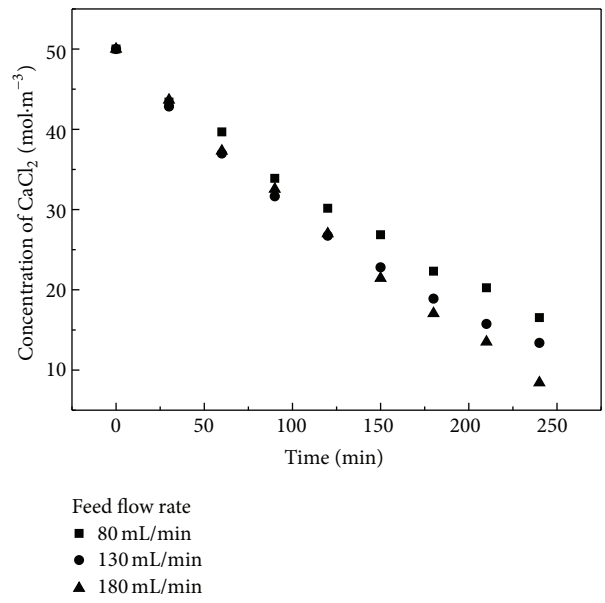

Figure 8: Effect of feed flow rate on $CaCl_2$ removal from sugar solution. Process conditions of feed: 80 mL/min, 130 mL/min and 180 mL/min with $CaCl_2$ (50 mol·m^{-3}) in 5% sugar solution; anolyte: 830 mL/min with HCl (100 mol·m^{-3}); catholyte: 830 mL/min with Na_2EDTA (50 mol·m^{-3}) + AA (50 mol·m^{-3}); applied voltage: 8 V.

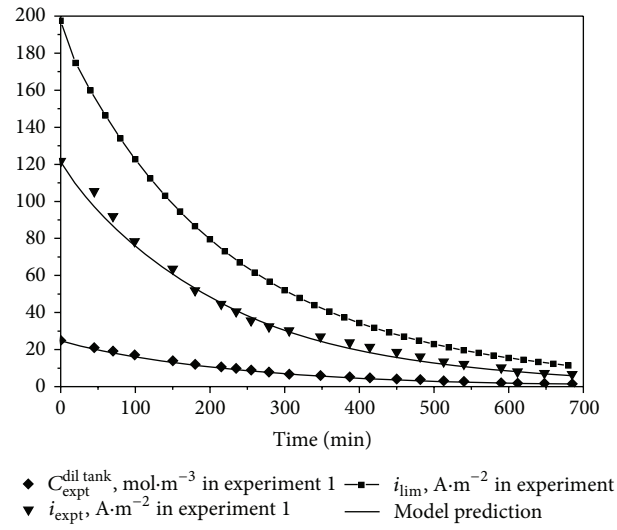

Figure 9: Plot of limiting current density, i_{lim} (A·m^{-2}), experimental current density, i (A·m^{-2}), and molar concentration of diluate tank, C_{expt}^{dilT} (mol·m^{-3}) (shown as discrete data points), versus time for a given set of operating condition: experiment 1 (feed flow rate = 130 mL·min^{-1}; anolyte = 100 mol·m^{-3} HCl; catholyte = 100 mol·m^{-3} NaOH; applied voltage = 4 V) [13]. Theoretically predicted values of current and concentration variation with time are shown by continuous line.

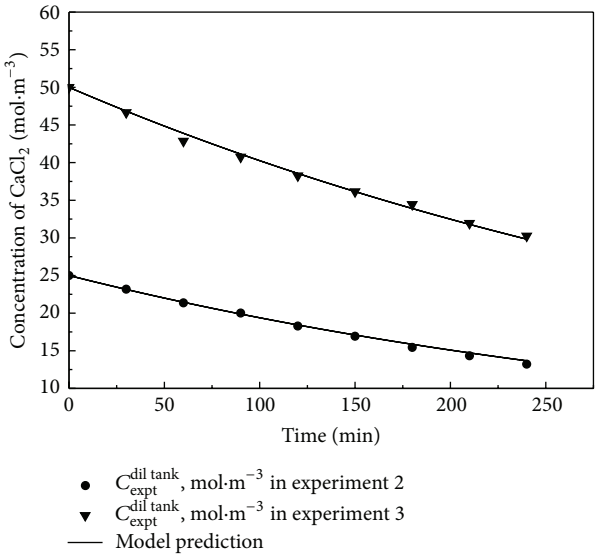

FIGURE 10: Close resemblance of theory (continuous line) with experimental molar concentration of $CaCl_2$ of the diluate tank (mol·m^{-3}) (discrete data points) versus time (min) for specified ED operating conditions: (i) experiment 2 (feed flow rate = 130 mL·min^{-1}; anolyte = 100 mol·m^{-3} HCl; catholyte = 25 mol·m^{-3} Na_2EDTA + 25 mol·m^{-3} AA; applied voltage = 4 V). (ii) Experiment 3 (feed flow rate = 130 mL·min^{-1}; anolyte = 100 mol·m^{-3} HCl; catholyte = 50 mol·m^{-3} Na_2EDTA + 50 mol·m^{-3} AA; applied voltage = 4 V) [13].

5.6. Role of Catholyte Composition and a Probable Mechanism for Smooth Operation of ED. $CaCl_2$ is a strong electrolyte and preferentially exists in ionized (Ca^{2+} and $2Cl^{-1}$) state in the aqueous solution containing sugar (5%). Water molecules form a hydration sphere around each dissociated ion and stabilize it. On application of external potential these hydrated species start crossing polar membranes charged with counter ions and cause concentration polarization buildup across the polar membrane.

The approach adopted here is to minimize the concentration polarization. Ca^{2+} ion crosses the cation exchange membrane. This was accomplished by either (i) precipitating out the ions or by (ii) complexing out before a back diffusion sets in. Two different catholyte streams were chosen with a definite purpose, for example, (i) 0.1 N NaOH (which forms an insoluble precipitate of Ca^{2+} ion (23)) and (ii) a mixture of acetic acid and di-sodium salt of EDTA (Na_2EDTA, a well-known complexing agent for bivalent cation (Ca^{2+}) after it crosses the CEM, (24)). Hydrated Ca^{2+} ions cross cation exchange membrane (CEM) and reaches catholyte compartment where it may precipitate or dissolve based on the electrolyte (s) and pH of the catholyte stream. Ca^{2+} ions react with the NaOH of catholyte stream and forms $Ca(OH)_2$. As the solubility product of $Ca(OH)_2$ in water is very low (~10^{-6}), it experiences high probability of precipitation over membrane surface facing higher pH. Once this precipitate comes in contact with electrolyte containing Na_2EDTA, it reacts and forms a stable complex, $CaNa_2EDTA$, which washes out the precipitate formed and cleans the membrane surface. The scheme of overall reaction is presented as follows:

$$Ca^{2+} + 2\left(OH^{-}\right) \longrightarrow Ca\left(OH\right)_2 \xrightarrow{CO_2} CaCO_3 + H_2O \quad (24)$$

$$Ca^{2+} + Na_2EDTA \longrightarrow CaNa_2EDTA + 2H^{+} \quad (25)$$

Bivalent cation are well known for their low solubility at high pH and often precipitate out as metal hydroxides [27]. This precipitation problem was also observed with calcium ion reported here when NaOH was used in catholyte stream. Figure 11 shows NaOH (100 mol·m^{-3}) as catholyte streams although increases ion removal rate initially, but vigorous fouling prevented the process from running for long duration. With NaOH as catholyte, $Ca(OH)_2$ precipitation was extensive which turned the membrane color from brownish yellow to white and probably blocked the swollen membrane pores on the rare side. Although this approach completely arrested the reverse transport of Ca^{2+} ions but continuous operation was limited due to membrane fouling, increased resistance, and drop in current density. Frequent acid wash helped in improving the membrane performance but continuous operation was not feasible.

Formation of white solid powder was noted over the membrane (CEM) surface facing catholyte stream (NaOH, higher pH) in experiment 1 and experiment 3. The white powder over membrane was investigated further to have better understanding of the problem which arose after ED operation for specified duration. Quantitative estimations of the fouled membrane were made by gravimetric method. The CEM membrane after ED experimentation was taken out, washed, and weighed, after drying and equilibration. The used membrane (equilibrated 24 hours at 100°C) was found to increase in mass over its initial mass (equilibrated) before ED. Gain of mass in used membrane is reported in Table 4.

The white deposit on the membrane surface could be removed by immersing the membrane in a dilute HCl (10% in water) solution. Immediately after immersion bubbling from the fouled surface of the membrane was observed. For complete dissolution of the white deposit, the membrane was left immersed in the solution for ~30 minutes until bubbling stopped. Subsequently the membrane was removed, washed repeatedly with deionized water, and dried in oven (100°C for 24 hours) and weighed. A blank test was simultaneously performed using a fresh membrane to record the difference between used and fresh membrane. For an applied potential the dry mass of the used membrane was found to be dependent on its duration of application, electrolyte concentration, and electrolyte stream pH.

Multiple samples of the used membrane were tested and formation of bubbles was confirmed. Once the bubbling stopped after immersing the membrane in dilute HCl solution, the piece was taken out, washed, dried, and equilibrated before weighing. Mass of the membrane did not deviate much from its initial value. This indicated possibility of CO_2 evolution from the reaction of HCl with $CaCO_3$. The most probable sequence of the overall reaction occurring over the

Table 4: Specific energy consumption, mass transfer coefficient, average running cost estimated, and gravimetric analysis.

Expt.	Specific energy consumption for $CaCl_2$ removal, E_{sp} (kWh·kg^{-1})	Average running cost (INR/g of $CaCl_2$ removed)	Mass transfer coefficient, k (m·s^{-1}) × 10^5	% weight gained by CEM due to fouling
1	2.4023	4.7	1.928	22
2	2.4027	3.4	1.174	3
3	2.4027	1.9	1.173	17

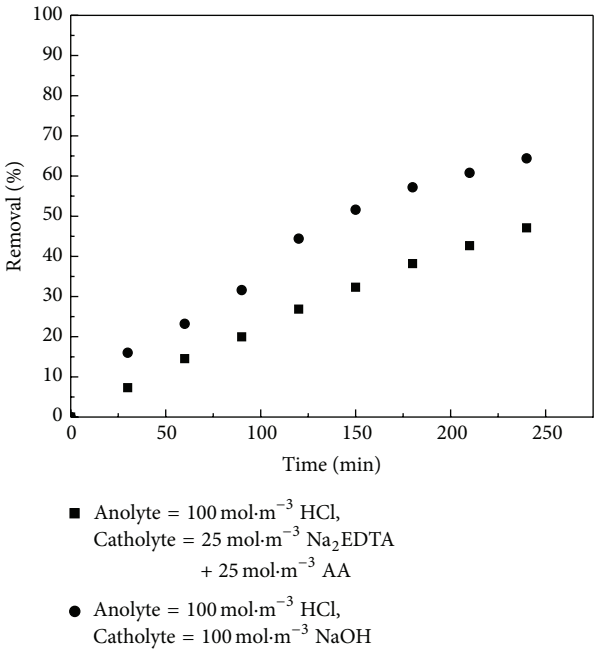

Figure 11: Comparison of Ca^{2+} ions (feed solution, 25 mol·m^{-3}) removal rate between two different techniques adopted. Case 1: anolyte = 100 mol·m^{-3} HCl; catholyte = 100 mol·m^{-3}NaOH. Case 2: anolyte = 100 mol·m^{-3} HCl; catholyte = 25 mol·m^{-3} Na_2EDTA + 25 mol·m^{-3} AA [13].

membrane surface and its subsequent cleaning with dilute HCl may be explained by the following scheme:

$$CO_2\ (\text{air}) + 2OH^- \longrightarrow {CO_3}^{2-} + H_2O \quad (26)$$

$$Ca(OH)_2 + CO_2 \longrightarrow CaCO_3\ (\text{s}) + H_2O \quad (27)$$

$$CaCO_3\ (\text{s}) + HCl \longrightarrow CaCl_2 + CO_2\ (\text{g}) + H_2O \quad (28)$$

At higher pH, solubility of CO_2 (air) increases in NaOH solution (catholyte stream) which results in formation of ${HCO_3}^{-1}/{CO_3}^{2-}$. These ions subsequently react with NaOH to form Na_2CO_3 providing the source for $CaCO_3$ precipitation from $Ca(OH)_2$. Conversion of $Ca(OH)_2$ to ${CO_3}^{-2}$ is (27) is thermodynamically favorable and moves forward. Nearly 1000 times higher value of solubility product of $Ca(OH)_2$ [5.5×10^{-6}] over $CaCO_3$ [3.39×10^{-9}] [28] drives the process faster.

Formation of $CaCO_3$ not only increased membrane resistance to ion transport but also made the ED operation discontinuous. The process was made uninterrupted by changing the electrolyte composition of the catholyte stream. Here we report application of Na_2EDTA-acetic acid solution as catholyte stream; the chelating agent continuously complexes with the precipitated $CaCO_3$ and formed corresponding salt $CaNa_2$EDTA. The pH of catholyte stream was adjusted between 3.5–5.0 (Table 2) and the anolyte was maintained as HCl (100 mol·m^{-3}). This combination showed negligible fouling even after long (240 min) operation time (Table 4).

The mass transfer coefficients estimated from Sherwood number correlation (11) showed higher values while NaOH (100 mol·m^{-3}) was used as catholyte stream compared to Na_2EDTA-acetic acid (AA) combination (Table 4). Reduced mass transfer coefficient with Na_2EDTA-acetic acid stream may be attributed to higher solution resistance arising possibly due to weak dissociation of acetic acid of Na_2EDTA + AA combination than that of NaOH. The dissociation constant can get further affected due to Na_2EDTA (a bulky diffusing species). Thus, reduction in mass transfer coefficient lowered Ca^{2+} ion removal rate.

As of now, we have understood that chemical composition and concentration of anolyte/catholyte streams play crucial role in controlling overall resistance and ion removal rate. The specific energy consumption, E_{sp}, estimated from (23) (Table 4) shows lower value with NaOH compared to the streams containing Na_2EDTA + AA.

The average running cost to remove unit mass of $CaCl_2$ is reported in Table 4. The cost is dependent on concentration of the electrolyte stream and time of ED operation. Cost is inversely proportional to initial concentration of the stream and directly proportional to operation time. Energy due to pumping is the major contribution to the overall costs estimate in a batch ED operation for a given time.

6. Conclusions

Calcium ion ($CaCl_2$, 25 mol·m^{-3}) removal rate depends on feed flow rates, electrolyte (anolyte/catholyte) components, concentrations, applied potential, and so forth. NaOH as catholyte showed higher removal rate and increased mass transfer coefficient over mixed electrolyte (AA-Na_2EDTA). Specific energy consumption (E_{sp}, kWh·kg^{-1}) estimates for three typical set of experiments (Table 4) also support the above observation of easy ion removal rate. Based on this it may be concluded that although NaOH shows better performance for the duration chosen in this report, but an uninterrupted mode ED operation would be feasible with mixed electrolyte only but of course energy consumption will be partly increasing. The unsteady state model used could

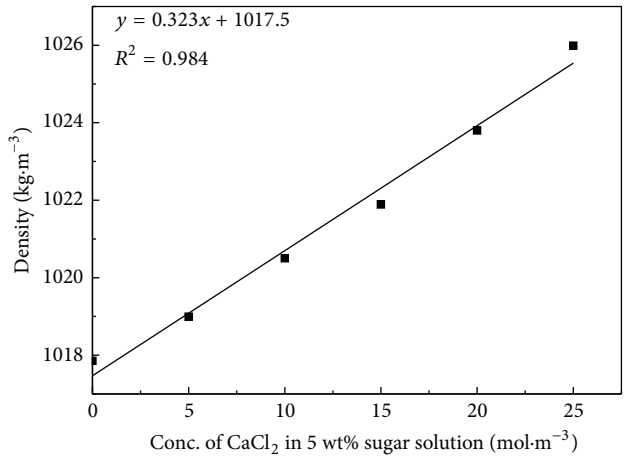

FIGURE 12: Calibration chart used to estimate solution density (kg·m^{-3}) from molar concentration of $CaCl_2$ (mol·m^{-3}) in 5 wt% sugar solution.

effectively predict the current density and concentration change with an accuracy of 95%.

Appendix

Density values of 5% sugar solution with varying concentration of $CaCl_2$ were estimated from the fitted equation (Density (kg·m^{-3}) = 0.323 × Concentration (mol·m^{-3}) + 1017.5; R^2 = .98) obtained from the experimental data of density versus concentration of $CaCl_2$ in 5% sugar solution (Figure 12).

Nomenclature

List of Symbols

a: Sh number empirical equation constant
A_m: Area of the membrane, m^2
b: Sh number empirical equation constant
c: Sh number empirical equation constant
C: Concentration, mol·m^{-3}
D: Diffusivity of the salt or ion in the solution at temperature, T
D°: Diffusivity of the salt or ion at infinite dilution at temperature, T
D_j: Diffusivity of ion "j"
E_{el}: Electrode potential, V
E_{tot}: Total electric potential applied, V
E_{sp}: Specific energy consumption, kWh·kg^{-1}
F: Faraday constant, C·gm-eq^{-1}
i: Current density, A·m^{-2}
$i_{j,lim}$: Limiting current density of ion "j"
I: Ionic strength
J: Current, A
k: Mass transfer coefficient, m/s
L: Characteristic length, m
m_j: Molality of ion "j"
Q: Volumetric flow rate, m^3·s^{-1}
R: Gas constant, J·kg^{-1}·K^{-1}
$R_{anolyte}$: Resistance of anolyte chamber
$R_{catholyte}$: Resistance of catholyte chamber
$R_{diluate}$: Resistance of diluate chamber
R_{tot}: Total Resistance of the electrodialysis cell
Re: Reynolds number
Sc: Schmidt number
Sh: Sherwood number
t: Time, s
T: Temperature, K
$t_{+,CEM}$: Transport number of cation in cation exchange membrane
$t_{-,AEM}$: Transport number of anion in anion exchange membrane
$t_{j,m}$: Transport number of ion "j" in the membrane
$t_{j,b}$: Transport number of ion "j" in the bulk solution
v: Velocity, m/s
V: Volume, m^3
z: Ion charge.

Subscripts

AEM: Anion exchange membrane
b: Bulk solution
CEM: Cation exchange membrane
C: Compartment
j: Ion, "j"
T: Feed tank
±: Cation or anion.

Superscripts

Conc: Concentrate
dil: Diluate
lim: Limiting.

Greek Symbols

η: Current efficiency
ε: Applied voltage, V
μ: Viscosity of the solution at the same temperature T, Pa·s
μ°: Viscosity of the pure water at a temperature T, Pa·s
Λ: Conductivity, S
λ_+, λ_-: Limiting (zero concentration) ionic conductance, (A·cm^{-2})·(V·cm^{-1})(g-eqv·cm^{-3})
ρ: Density, kg·m^{-3}
δ: Diffusion boundary layer thickness, m
ξ: Potential gradient, V·m^{-1}
ψ: Potential drop in the diffusion boundary layer, V
$\gamma_\pm$: Mean ionic activity coefficient.

Conflict of Interests

The authors declare that there is no conflict of interests regarding to the publication of this paper.

Acknowledgment

Financial support to execute the experimental work is gratefully acknowledged to IIT Roorkee (no. IITR/SRIC/244/FIG-Sch-A).

References

[1] R. B. L. Mathur, *Handbook of Cane Sugar Technology*, Oxford and IBH Publishing, New Delhi, India, 1978.

[2] F. Smagghe, J. Mourgues, J. L. Escudier, T. Conte, J. Molinier, and C. Malmary, "Recovery of calcium tartrate and calcium malate in effluents from grape sugar production by electrodialysis," *Bioresource Technology*, vol. 39, no. 2, pp. 185–189, 1992.

[3] A. Elmidaoui, L. Chay, M. Tahaikt et al., "Demineralisation of beet sugar syrup, juice and molasses using an electrodialysis pilot plant to reduce melassigenic ions," *Desalination*, vol. 165, p. 435, 2004.

[4] G. Trägårdh and V. Gekas, "Membrane technology in the sugar industry," *Desalination*, vol. 69, no. 1, pp. 9–17, 1988.

[5] H. Strathmann, *Ion-Exchange Membrane Separation Processes*, Elsevier, 2004.

[6] J. J. Krol, M. Wessling, and H. Strathmann, "Concentration polarization with monopolar ion exchange membranes: current-voltage curves and water dissociation," *Journal of Membrane Science*, vol. 162, no. 1-2, pp. 145–154, 1999.

[7] V. Geraldes and M. D. Afonso, "Limiting current density in the electrodialysis of multi-ionic solutions," *Journal of Membrane Science*, vol. 360, no. 1-2, pp. 499–508, 2010.

[8] H. Strathmann, J. J. Krol, H.-J. Rapp, and G. Eigenberger, "Limiting current density and water dissociation in bipolar membranes," *Journal of Membrane Science*, vol. 125, no. 1, pp. 123–142, 1997.

[9] H.-J. Lee, H. Strathmann, and S.-H. Moon, "Determination of the limiting current density in electrodialysis desalination as an empirical function of linear velocity," *Desalination*, vol. 190, no. 1–3, pp. 43–50, 2006.

[10] Y. Tanaka, "Limiting current density of an ion-exchange membrane and of an electrodialyzer," *Journal of Membrane Science*, vol. 266, no. 1-2, pp. 6–17, 2005.

[11] A. Elmidaoui, F. Lutin, L. Chay, M. Taky, M. Tahaikt, and M. R. A. Hafidi, "Removal of melassigenic ions for beet sugar syrups by electrodialysis using a new anion-exchange membrane," *Desalination*, vol. 148, no. 1–3, pp. 143–148, 2002.

[12] Y. Tanaka, "Irreversible thermodynamics and overall mass transport in ion-exchange membrane electrodialysis," *Journal of Membrane Science*, vol. 281, no. 1-2, pp. 517–531, 2006.

[13] S. Chattopadhyay, *Removal of Calcium Ion from Sugar Solution through Electrodialysis*, Department of Chemical Engineering, Indian Institute of Technology Kanpur, Kanpur, India, 1994.

[14] B. E. Poling, J. M. Prausnitz, and J. P. O'Connell, *The Properties of Gases and Liquids*, McGraw-Hill, New York, NY, USA, 5th edition, 2000.

[15] L. Yuan-Hui and S. Gregory, "Diffusion of ions in sea water and in deep-sea sediments," *Geochimica et Cosmochimica Acta*, vol. 38, no. 5, pp. 703–714, 1974.

[16] http://www.sugartech.co.za/viscosity/index.php.

[17] M. S. Isaacson and A. A. Sonin, "Sherwood number and friction factor correlations for electrodialysis systems, with application to process optimization," *Industrial & Engineering Chemistry Process Design and Development*, vol. 15, no. 2, pp. 313–321, 1976.

[18] J. M. Ortiz, J. A. Sotoca, E. Expósito et al., "Brackish water desalination by electrodialysis: batch recirculation operation modeling," *Journal of Membrane Science*, vol. 252, no. 1-2, pp. 65–75, 2005.

[19] F. S. Rohman, M. R. Othman, and N. Aziz, "Modeling of batch electrodialysis for hydrochloric acid recovery," *Chemical Engineering Journal*, vol. 162, no. 2, pp. 466–479, 2010.

[20] R. E. Treybal, *Mass-Transfer Operations*, McGraw-Hill, New York, NY, USA, 3rd edition, 1980.

[21] R. B. Bird, W. E. Stewart, and E. N. Lightfoot, *Transport Phenomenon*, John Wiley & Sons, 2nd edition, 2002.

[22] J. Balster, M. H. Yildirim, D. F. Stamatialis et al., "Morphology and microtopology of cation-exchange polymers and the origin of the overlimiting current," *The Journal of Physical Chemistry B*, vol. 111, no. 9, pp. 2152–2165, 2007.

[23] O. V. Grigorchuk, V. I. Vasil'eva, and V. A. Shaposhnik, "Local characteristics of mass transfer under electrodialysis demineralization," *Desalination*, vol. 184, no. 1–3, pp. 431–438, 2005.

[24] V. M. Barragán and C. Ruíz-Bauzá, "Current-voltage curves for ion-exchange membranes: a method for determining the limiting current density," *Journal of Colloid and Interface Science*, vol. 205, no. 2, pp. 365–373, 1998.

[25] J. Koryta, J. Dvorak, and L. Kavan, *Principles of Electrochemistry*, John Wiley & Sons, New York, NY, USA, 2nd edition, 1993.

[26] N. Kabay, M. Demircioglu, E. Ersöz, and I. Kurucaovali, "Removal of calcium and magnesium hardness of electrodialysis," *Desalination*, vol. 149, no. 1–3, pp. 343–349, 2002.

[27] M. Araya-Farias and L. Bazinet, "Electrodialysis of calcium and carbonate high-concentration solutions and impact on membrane fouling," *Desalination*, vol. 200, no. 1–3, p. 624, 2006.

[28] http://www4.ncsu.edu/~franzen/public_html/CH201/data/Solubility_Product_Constants.pdf.